Subcellular localization of microcystin in the liver and the gonad of medaka fish acutely exposed to microcystin-LR

Qin Qiao[1], *Chakib Djediat*[1], *Hélène Huet*[1,2], *Charlotte Duval*[1], *Séverine Le Manach*[1], *Cécile Bernard*[1], *Marc Edery*[1], *Benjamin Marie*[1,*]

[1] UMR 7245 MNHN/CNRS Molécules de Communication et Adaptation des Micro-organismes, Sorbonne Universités, Muséum National d'Histoire Naturelle, CP 39, 12 Rue Buffon, 75005 Paris, France.

[2] Ecole Nationale Vétérinaire d'Alfort, Université Paris-Est, BioPôle Alfort, 94700 Maisons-Alfort, France.

* Corresponding author. UMR 7245 MNHN/CNRS Molécules de Communication et Adaptation des Micro-organismes, Sorbonne Universités, Muséum National d'Histoire Naturelle, CP 39, 12 Rue Buffon, 75005 Paris, France. Tel.: +33 1 40 79 32 12

E-mail address: bmarie@mnhn.fr (B. Marie)

Abstract

Among the diverse toxic components produced by cyanobacteria, microcystins (MCs) are one of the most toxic and notorious cyanotoxin groups. Besides their potent hepatotoxicity, MCs have been revealed to induce potential reproductive toxicity in various animal studies. However, little is still known regarding the distribution of MCs in the reproductive organ, which could directly affect reproductive cells. In order to respond to this question, an acute study was conducted in adult medaka fish (model animal) gavaged with 10 $\mu g.g^{-1}$ body weight of pure MC-LR. The histological and immunohistochemical examinations reveal an intense distribution of MC-LR within hepatocytes along with a severe liver lesion in the toxin-treated female and male fish. Besides being accumulated in the hepatocytes, MC-LR was also found in the connective tissue of the ovary and the testis, as well as in oocytes and degenerative spermatocyte-like structures. Both liver and gonad play important roles in the reproductive process of oviparous vertebrates. This observation constitutes the first

observation of the presence of MC-LR in the reproductive cell of a vertebrate model with *in vivo* study. Our results, which provide intracellular localization of MC-LR in the gonad, advance our understanding of the potential reproductive toxicity of MC-LR in fish.

Keywords:

Microcystin; reproductive cell; immunogold electron microscopy; OATP; reproductive toxicity

1. Introduction

Recurrent cyanobacterial blooms frequently occur worldwide in eutrophic freshwaters. Various bloom-generating species of cyanobacteria can produce natural toxic components (cyanotoxins), and their blooms threaten human health as well as living organisms of the aquatic environment. Among cyanotoxins, microcystins (MCs) are the most prevalent cyanobacterial hepatotoxins, with 248 structural variants (Spoof and Catherine, 2017), being produced by at least six genera of cyanobacteria (Puddick et al., 2014). Among all these known variants, microcystin-LR (MC-LR) is considered to be the most common and potently toxic (Puddick et al., 2014).

MCs have difficulty to penetrate into vertebrate cells via passive transport due to their hydrophilic nature, and organic anion transporting polypeptides (OATPs) are known to be able to transport MCs through cell membranes (Campos and Vasconcelos, 2010). Once within the cell, MCs specifically inhibit eukaryotic serine/threonine protein phosphatases 1 and 2A, which causes the disruption of numerous cellular signals and processes (Fischer et al., 2005; MacKintosh et al., 1990). Although there have been 70 members of OATP superfamily identified in the database from humans, rodents and some additional species (Hagenbuch and Stieger, 2013), not all OATPs are capable to transport MCs through cell membranes. The capability of MC-transport has been demonstrated for OATP1A2 (mainly expressed in the vertebrate brain), liver-specific OATP1BA and OATP1B3 in humans (Fischer et al., 2005). In fish, liver-specific OATPs, such as OATP1d1 in little skate (Meier-Abt et al., 2007) and rtOATP1d1in rainbow trout (Steiner et al., 2014), have been reported to mediate

MC-transport. Different types of OATP distributed in different tissue or organs possess varying levels of affinities and capacities for different MC variants (Fischer et al., 2010, 2005; Steiner et al., 2016). Liver is the organ that presents the highest tropism for MCs (so-called "target"), since it is rich in a few liver-specific OATP members possessing high affinities and capacities to MCs. Several studies have reported the acute hepatotoxicity of MCs characterized by hepatocellular apoptosis (Zhang et al., 2013), necrosis (Mattos et al., 2014), intrahepatic hemorrhaging (Hou et al., 2015), and cytoskeleton disruption (Zhou et al., 2015). Additionally, the distribution of MCs in the liver has been detected using immunohistochemical methods in mice (Guzman and Solter, 2002; Yoshida et al., 1998) and fish (Djediat et al., 2011; Fischer and Dietrich, 2000; Marie et al., 2012).

In addition to liver, MCs have been documented to distribute and accumulate in various fish organs including intestine, kidney, gill and gonad (Acuña et al., 2012; Djediat et al., 2010; Mezhoud et al., 2008; Trinchet et al., 2013, 2011). Among these organs, the gonad could be considered as a secondarily most important target of MCs, as several field studies reported also the presence of MCs in the gonad of fish. For instance, in Lake Pamvotis (Greece), the gonad of common carp (*Cyprinus caprio*) was reported to contain about 50 ng eq. MC-LR g^{-1} body weight (bw) using ELISA test (Papadimitriou et al., 2012), and in Lake Taihu (China), three variants of MC (MC-LR, -YR and -LR) were determined in the gonad of various fish species using a liquid chromatography-electrospray ionization-mass spectrum system (LC-ESI-MS). Particularly, silver carp (*Hypophthalmichthys molitrix*) and goldfish (*Carassius auratus*) were observed to contain high concentrations of MCs in the gonad (60 and 150 ng MCs g^{-1} DW, respectively) (Chen et al., 2009). In laboratories, the distribution of MC-LR in the gonad of medaka fish administered with pure toxin was also testified using a radiotracing method (Mezhoud et al., 2008). Although the accumulation of MCs in the gonad has been documented previously through different methods, little is known about the localization of MCs within the gonad tissue, or about the intracellular distribution of MCs. Only one field study reported the presence of MCs in the gonadal somatic tissue, but apparently not in the oocytes in common bream

(*Abramis brama*) using immunohistochemical method (Trinchet et al., 2013). To date, it is still hard to know whether MC could enter the reproductive cells or only accumulate in the conjunctive tissue of gonad. Although not the most sensitive detection method, the immunohistochemical examination is a well-established way of providing the precise subcellular localization of MCs in the gonad, which could largely advance our current knowledge of the directly toxic effects of MCs on the gonad.

In the present study, in order to investigate subcellular distribution of MCs in fish gonads, an immunohistochemical assay with light microscopy and electron microscopy was conducted in adult medaka fish that were gavaged with acute doses of MC-LR (10 $\mu g.g^{-1}$ bw of MC-LR, 1 h exposure). Localization of the toxin in the gonad was showed by MC-LR-specific antibodies, MC10E7, that specifically binds to the arginine at position 4 of MC-LR (Zeck et al., 2001). In addition, the toxin distribution and histopathological change in the liver (the first target of MCs) were also investigated in order to compare the toxic effect in liver and gonad.

2. Materials and methods

2.1 Chemical and reagent

MC-LR, purchased from Novakit® (Nantes, France), was selected as the model MC for the present experiment. Five hundred µg of MC-LR was dissolved in 500 µL of ethanol and 500 µL of water. The ethanol was evaporated with a Speedvac. The concentration of MC-LR in the obtained solution was quantified using a commercial Adda-specific AD4G2 ELISA test (Abraxis), and then adjusted to be 1 $\mu g.\mu L^{-1}$.

2.2 Fish maintenance, exposure and sampling

The experimental procedures were conducted in accordance with the European Union regulations and the supervision of the Cuvier's ethical committee of the Museum National d'Histoire Naturelle (MNHN) concerning the protection of experimental animals. Five-month-old medaka fish (*Oryzias latipes*) of the inbred Cab strain maintained in the lab was used for this experiment. Female and male fish were maintained in 2 glass aquaria, respectively, filled with a mixture of tap water and

reverse osmosis filtered water (1:2) in a flow-through system for aeration and filtration, in a temperature controlled room (25 ± 1 °C), with a 12 h:12 h light:dark cycle. Fish were fed three times a day with commercial dry bait for juvenile salmons.

Eight females and eight males were randomly selected from the aquaria. The fish were anesthetized with tricaine (150 $mg.L^{-1}$) before gavage. Five females and five males were gavaged with 5 µL of MC-LR solution (1 $\mu g.\mu L^{-1}$) per fish, representing about 10 $\mu g.g^{-1}$ bw of MC-LR (average body weight is 0.52 g, the body weight of individual fish is shown in Supplementary table 1). This concentration is modified according to a few previous studies in which medaka fish exhibited noticeable tissue damage and toxin presence in liver upon exposure to 5 $\mu g.g^{-1}$ bw of MC-LR (Djediat et al., 2011, 2010). Two females and two males were gavaged with 5 µL water as the non-toxin control, and 1 female and 1 male without any treatment were used as the non-gavage control. After 1 h oral exposure, fish were anesthetized with tricaine, sacrificed, and the liver and gonad were collected on ice. One tissue was cut into 2 parts, one part was immediately fixed with formaldehyde fixing solution (Supplemental material 1) according to the protocol provided by the histopathological platform of Ecole Nationale Vétérinaire d'Alfort (ENVA), and the other part was fixed with paraformaldehyde fixing solution (Supplemental material 2) following the instruction of the electron microscopy platform of Muséum National d'Histoire Naturelle (MNHN).

2.3 Histopathological observation and immunolocalization of microcystins

In the platform of ENVA, the liver and gonad samples fixed in formaldehyde fixing solution at 4 °C for 48 h were dehydrated in successive baths of ethanol (from 70 to 100%) and embedded in paraffin. Blocks were cut into 4 µm thick sections. The sections of each sample were deposited on 3 slides. One slide was stained with hematoxylin-eosin-saffron (HES) staining for histopathological observation. Another slide (only liver sample) was stained with periodic acid-Schiff (PAS)/Alcian blue staining for the assessment of hepatic glycogen reserve. The glycogen reserve analysis performed by ImageJ software (version 1.51d) estimated the hepatic glycogen quantity as a surface percentage of the purple-red pixels on 5 randomly selected

151 photos (200 × magnification, photo size 1388×1040 pixels, as seen in Figure 1) per
152 individual. The last slide, for immunolocalization of MC, was incubated with a
153 monoclonal antibody to MC-LR (MC10E7, Alexis) that recognizes all MCs with Arg
154 in position 4 (dilution 1:4000). The immunolabeling was routinely performed with an
155 automated Module Discovery XT (Ventana, Tuscon, USA) using a colorimetric
156 peroxidase-specific staining with diaminobenzidine (DAB), a substrate that produces
157 a highly insoluble brown precipitate. The slides were counterstained with hematoxylin
158 in the end. The secondary antibody control sections were prepared by skipping the
159 first antibody MC10E7 incubation step. One MC-contaminated medaka liver sample
160 from an acute high dose exposure in the lab previously was included as the technically
161 positive control.

162 In the platform of MNHN, the liver and gonad samples fixed in
163 paraformaldehyde fixing solution at 4 °C overnight were dehydrated in successive
164 baths of ethanol (from 30 to 100%) and embedded into the Unicryl resin. Blocks were
165 cut into 0.5 μm-thick semi-thin sections (stained with toluidine blue staining) and 60
166 nm-thick ultrathin sections for histopathological observation and immunolocalization
167 of MC with electron microscopy, respectively. The 60 nm-thick ultrathin sections
168 were collected by gold grids. Then, the sections were incubated with the same
169 primary antibodies (MC10E7) at 4 °C overnight and rinsed, then incubated with a
170 secondary antibody coupled to gold nanoballs (6 or 10 nm of diameter) at room
171 temperature for 1 h. After being well rinsed with distilled water, the sections were
172 stained with a saturated solution of uranyl acetate in 50% ethanol and then observed
173 under an H-7700 Hitachi (Tokyo, Japan) transmission electron microscope.
174

175 **3. Results**

176 During the 1 hour of post-gavage, all MC-treated fish exhibit abnormal
177 swimming behaviors, such as difficulty in moving or losing body balance. In the
178 contrary, the fish of control group all swim normally. Histopathological and
179 immunohistochemical observation results of each individual are summarized in Table
180 1, which shows visible toxic effects and clear toxin distribution in nearly every

MC-treated fish, but not in any control fish.

Table 1 Histopathological and immunohistochemical observation of each individual liver and gonad

Group		Fish [a]	Post-gavage	Histopathology (Liver)		Anti-MC-LR labeling [d]		
				Light microscopy		Light microscopy		Electron microscopy
				Liver damage [b]	Glycogen reserve (%) [c]	Liver	Gonad	Gonad
10 μg.g^{-1} b.w. of MC-LR		F01	1 h	+	23%	++	+	++
		F03	1 h	++	22%	++	+	+
		F04	1 h	+	15%	++	+	++
		F07	1 h	++	12%	++	+	++
		F10	1 h	+	1%	++	+	n.o.
		M02	1 h	+	0%	++	0	++
		M05	1 h	++	20%	++	+	++
		M06	1 h	+	2%	++	+	n.o.
		M08	1 h	+	26%	++	0	+
		M09	1 h	+	6%	++	+	++
Control	Non-toxin	F12	1 h	0	22%	0	0	0
		F14	1 h	0	50%	0	0	0
		M13	1 h	0	16%	0	0	0
		M11	1 h	0	25%	0	0	0
	Non-gavage	F16	1 h	0	49%	0	0	0
		M15	1 h	0	47.2	0	0	0

[a] F and M indicate female and male fish, respectively. [b] "++" indicates a severe liver damage, characterized by a large proportion of round hepatocytes, significant mitosis arrest, and obvious cell lysis and disjunction. "+" indicates a moderate liver damage, characterized by a large proportion of round hepatocytes, and a small area of cell lysis and disjunction. "0" indicates the normal liver structure. [c] indicates the percentage of glycogen reserve in the liver, the calculation formula: the area of the purple-red pixels ÷ the area of the whole image (1388×1040 pixels) × 100%. [d] "++" indicates strong and widely distributed immunolabelings, "+" indicates only a few immunolabeling spots, "0" indicates no immunolabeling, and "n.o." indicates not observed.

3.1 Histopathological effects with light microscopy

In the liver of all control fish, hepatocytes present compact and characteristic cord-like parenchymal organization and a distinctive central nucleus with a prominent nucleolus (Figure 1 A and B). The cytoplasm of hepatocytes contains mainly

glycoprotein and/or glycogen stores that are intensively stained in red-purple with PAS staining (Figure 1 E and F). In contrast, the livers of MC-LR treated fish exhibit noticeable tissue lesions characterized by a disintegration of the parenchymal organization and significant cell lysis. The hepatocytes all lose their polyhedral shape and become rounded and swollen. Within the hepatocytes, the reserve vesicles disappear, the cytoplasm presents various small bubble-like structures, and the nuclear chromatin becomes dense. Some hepatocytes exhibit a breakdown of the nuclear membrane, mitosis arrest, and dilation of endoplasmic reticulum (Figure 1 C and D). In addition, the hepatic intracellular glycoprotein and/or glycogen quantity seems to decrease, and the mean values of glycogen percentage for female controls, male controls, female toxin-treated fish and male toxin-treated fish are 15%, 11%, 40% and 29%.

For the gonad, there is no apparent cellular difference between the toxin-treated fish and the control ones.

3.2 Immunolocalization of MC-LR in the liver and the gonad

Through light microscopy, all livers of MC-LR treated fish exhibit a strong positive signal of MC-LR specific antibodies (Figure 2 A) whereas the secondary antibody control does not display any positive signal (Figure 2 B), being similar to control fish in which no immunolabeling is observed (Figure 2 G). For the toxin treated fish, the brown immunolabelings are evenly distributed in hepatocytes, but not in erythrocytes which are only stained in blue by hematoxylin. Within hepatocytes, the immunolabeling of MCs is showed in the cytoplasm and more intense labeling is observed in nuclei (Figure 2 A). Immunogold electron microscopy also shows that the black nanoballs (immunolabelings) are localized in the cytoplasmic inclusion and the nucleus (Figure 3 C) of hepatocytes of MC-LR treated fish, being particularly intense in the lysis area (Figure 3 B). MC-LR is also distributed intensely in residual bodies of the macrophage (Figure 3 D), whereas no immunolabeling is observed in the control fish (Figure 3 A) or in the secondary antibody control sections.

By light microscopy observation of the ovary of toxin-treated fish, clear immunolabelings are detected in the connective tissue and some round cells with

above 10 μm in diameter, being probably the early stage of oocyte (Figure 2 C), whereas the secondary antibody control does not display any positive signal (Figure 2 D), being similar to the control fish in which no immunolabeling is observed (Figure 2 H). Moreover, electron microscopy shows that the immunogold labelings are not only present in the gonadal somatic cells, but also distributed intensively in the chorion of oocytes (Figure 3 F), being less intense in the yolk vesicles and cytoplasm of oocytes (Figure 3 H), whereas no immunolabeling is observed in either the control fish (Figure 3 E and G) or the secondary antibody control sections.

On light microscope, weaker immunolabelings are found in the testicular connective tissue of a few toxin-treated male fish (Figure 2 E), whereas the secondary antibody control does not display any positive signal (Figure 2 F), being similar to the control fish in which no immunolabeling is observed (Figure 2 I). Immunogold electron microscopy shows a remarkable labeling in some round unidentified structures, being probably some degenerated germ cells (Figure 3 J), as well as in the connective tissue of certain area nearby seminiferous tubules (Figure 3 K), whereas no immunolabeling is observed in either the control fish (Figure 3 I) or the secondary antibody control section.

4. Discussion

MC-treated female and male fish in this study show the characteristic hepatocellular changes and the depletion of glycogen reserve that have been observed previously in fish (Djediat et al., 2011; Fischer et al., 2000; Fischer and Dietrich, 2000; Marie et al., 2012; Mezhoud et al., 2008) and mice (Guzman and Solter, 2002; Yoshida et al., 2001, 1998) acutely administered with MCs or MC-containing cyanobacteria extracts. In fact, the observed liver damage in the present study is also similar to some of those described in the fish after chronic intoxication with MCs (Acuña et al., 2012; Qiao et al., 2016; Trinchet et al., 2011). Trinchet and her colleagues observed an increase in rough endoplasmic reticulum in hepatocytes of medaka fish chronically exposed to MC-LR (5 $\mu g.L^{-1}$, 30 d), which is also found in the male toxin-treated medaka in the present study. This could be associated with the

induction of detoxification process. Another chronic in-house study reported a noticeable hepatic glycogen store depletion in medaka fish upon exposure to MC-LR (5 $\mu g.L^{-1}$, 28 d) (Qiao et al., 2016), which is consistent with the acute intoxication effect of MC-LR observed here, and the increased energy needs for the MC detoxification process might be the cause.

Severe liver damages are often accompanied by remarkable accumulation of MCs in the liver. The present study shows an intense distribution of MC-LR in the lytic hepatocyte of the toxin-treated medaka fish through the immunohistochemistry. MCs have been reported to mostly localize in the cytoplasm of hepatocytes where they disturb a sequence of phosphorylation/dephosphorylation-dependent biochemical reactions, resulting in the disruption of multiple cellular processes, and consequently causing the deformation of hepatocytes, apoptosis and lysis (Campos and Vasconcelos, 2010). Furthermore, a high concentration of MC-LR is also observed in the hepatic nucleus here, which is consistent with the result provided in a few previous acute studies (Fischer et al., 2000; Guzman and Solter, 2002; Yoshida et al., 1998). Protein phosphatases PP1 and PP2A, one of the main molecular "target" of MCs, localize in both nucleus and cytoplasm (Shenolikar, 1994). Therefore, the observed nuclear accumulation of MC-LR could be the consequence of the MC specific antibodies binding to the MC-LR-PP1/PP2A adducts localized in the nucleus.

In the present study, MC-LR is also observed to be present in the gonad of MC-treated fish. For females, MC-LR is localized in the connective tissue of ovary, as well as in some maturing oocytes. The presence of MC in the connective tissue of fish ovary has been reported previously in common bream collected from MC-contaminated lakes (Trinchet et al., 2013). It seems that MCs are transported through the bloodstream into gonads, in which they can firstly accumulate in the connective tissue, and then transported into various gonadal somatic cells, even reproductive cells. Our result indeed exhibits an apparent distribution of MC-LR in the oocyte of vertebrates with *in vivo* condition for the first time, and the toxin is clearly localized in the yolk and the cytoplasm of the oocyte, being particularly highly

intensive in the chorion. Through the immunochemistry, MC was once reported to be present in the oocyte of snail upon exposure to MC-LR for 5 weeks (Lance et al., 2010). But it is unclear how MC-LR enters into oocytes since the oocyte plasma membrane seems to lack the OATPs possessing MC-transport capability. It can be assumed that MCs may be transported into oocytes as protein-bound forms along with protein import during oogenesis, since the exchange of a big amount of protein and other materials are occurring prior to complete chorion maturation, or even simply through the passive diffusion of a small quantity.

For MC-treated male fish, immunogold electron microscopy reveals an intense distribution of MC-LR in the connective tissue of the testis in some certain area, as well as in some degenerated spermatocyte-like structure. It is uncertain whether the observed degenerated structure is caused by the toxic effect of MC-LR, or is associated with the natural apoptotic loss, since a certain level of apoptosis or degeneration in germ cells is normal in fish testis (Schulz et al., 2010). The observed high accumulation of MCs in a certain area of connective tissue still implies a potential germ cell damage induced by MC exposure. The connective tissue of the testis consists of massive fibers and various types of gonadal somatic cells, such as Leydig cells and Sertoli cells. They are important functional cells in the testis, being responsible for synthesizing and secreting androgens that are essential for the development and maturation of germ cells or serving as channels for the transport of nutrients into the growing germ cells (Dietrich and Krieger, 2009). Therefore, the high accumulation of MC-LR in the connective tissue and its subsequent toxic effect on gonadal somatic cells may indirectly disturb normal spermatogenesis process, affecting the normal reproductive process. In the present study, we do not observe any histopathological modification in the spermatocyte of MC-treated fish, which seems to be due to the short exposure time (1h). In a previous in-house study, MC-LR has been reported to result in the disturbance of spermatogenesis in medaka fish following a chronic exposure (Trinchet et al., 2011). Considerable testicular injury and spermatocyte abnormality have been found in several species of vertebrate model

314 animals, such as mouse, rat and fish, upon exposure to MCs acutely or chronically (Li
315 et al., 2008; Su et al., 2016; X. Wang et al., 2013; Zhao et al., 2012; Zhou et al., 2013).
316 However, to date, according to *in vivo* studies using these vertebrate models, no
317 evidence regarding the incorporation of MCs into spermatocytes has been reported yet.
318 Only one study showed a clear distribution of MC-LR on the tubal wall of seminiferous
319 tubules of the MC-treated rats through the immunofluorescence method (injection
320 with 300 $\mu g.kg^{-1}$ bw of MC-L for 6 d) (L. Wang et al., 2013). In the present study,
321 MC-LR is not found in any clear spermatocytes of the toxin-treated fish through the
322 immunogold labeling technique, which is consistent with the common knowledge of
323 the organ distribution of the MC-transporting OATPs. The identified OATPs that
324 possess strong MC-transport capabilities are highly abundant in the liver, but hardly
325 known to be present in the cell membrane of reproductive cells. However, one *in vitro*
326 study reported that MC-LR was able to immigrate into isolated rat spermatogonia
327 (Zhou et al., 2012). Furthermore, in this study, at least 5 OATPs were detected at the
328 mRNA level in spermatogonia and their expression level was affected by MC-LR,
329 implying that these OATPs may involve in MC-transport into the reproductive cells.
330 Therefore, it is noteworthy that some unidentified OATPs which possess
331 MC-transport capabilities might be expressed in the reproductive cells at a relatively
332 low level. But the information regarding the unidentified MC-transporting OATPs
333 and their expression level in reproductive cells still remains very limited.

334 The present acute study indeed shows a clear subcellular distribution of MC-LR in
335 the gonad of the toxin-treated fish. However, in another in-house chronic study, MCs
336 were not detected in the ovary or testis of medaka fish following a balneation
337 exposure to 5 $\mu g.L^{-1}$ of MC-LR for 30 days by using the same immunolocalization
338 techniques (Trinchet et al., 2011). There are at least two causes that may account for
339 this discrepancy. Toxin concentration, detoxification process and exposure time are
340 crucial for such immunolabeling results. Ten $\mu g.g^{-1}$ bw of MC-LR used in the present
341 study is a quite high concentration (the highest LD_{50} value of MCs by i.p. injection is
342 about 1.5 $\mu g.g^{-1}$ bw in fish) (Malbrouck and Kestemont, 2006), and the short time of

exposure (1 h) largely reduced the possible toxin excretion process through liver detoxification, together leading to a sufficient quantity of toxin that could access to gonad through blood stream and be detected by the immunohistological method. Besides, it is worth to mention that the process of histological section preparation may affect the result, since a fraction of MC-LR (mainly free MC-LR) was removed during the dehydrating process of the section preparation. The immunostaining here indeed detects MC-LR-PP1/PP2A adducts mostly, due to the strong affinity of MC-LR to protein phosphatases PP1/PP2A (Yoshida et al., 2001). Dmet-Asp and D-Glu residues of MC-LR play important roles in forming the MC-LR-PP1/PP2A adducts (Campos and Vasconcelos, 2010).

5. Conclusion

Our histological and immunohistochemical results reveal that both liver and gonad are significantly affected by MC-LR exposure. An intense distribution of MC-LR within hepatocytes along with a severe liver damage attests to the potent hepatotoxicity of MC. The immunohistochemical results show that, besides being accumulated in the hepatocytes, MC-LR is also found in the connective tissue of the gonad, as well as in the reproductive cell (oocytes). This finding constitutes the first observation of the presence of MC in the reproductive cell in vertebrate model animals with *in vivo* condition. Both liver and gonad play important roles in the reproductive process of oviparous vertebrates. Our results of the present acute study, which provide a distinct subcellular localization of MC-LR in the liver and gonad, contributes to a better understanding of the potential reproductive toxicity of MC-LR at the histopathological level, favoring the characterization of underlying mechanisms. Meanwhile, the penetration of MCs into the reproductive cell suggests a possible transferring of MCs from adults into offspring which could cause a big issue for the population of aquatic organisms. The further investigation concerning this perspective is needed to advance our current knowledge of the protection of aquatic organism populations, as well as human beings from the widespread MCs in the freshwater

372 body.

373

374 **Acknowledgments**

375 This work was supported by grants from the CNRS Défi ENVIROMICS
376 "Toxcyfish" project and from the ATM "Cycles biologiques: evolution et adaptation"
377 of the MNHN to Dr. Benjamin Marie. Qin Qiao PhD is founded by the China
378 Scholarship Council. We thank the Amagen platform for providing medaka fish Cab
379 strain, the microscopy platform of ENVA and MNHN for the histopathology and
380 immunolocalization techniques. We also thank Marie-Claude Mercier for its
381 administrative support.

382 **Author Contribution**

383 Q.Q., C.D., H.H., C.B., M.E. and B.M. conceived the experiments, Q.Q., C.D., H.H,
384 C.D., S.L.M. and B.M. conducted the experiments, Q.Q., C.D., H.H and B.M.
385 analyzed the results. All authors reviewed the manuscript.
386 The authors declare no competing financial interest.

387

388 **List of Supplementary materials:**

389 Supplementary material 1. Formaldehyde fixing solution (100 mL) provided by the
390 platform of ENVA

391 Formaldehyde (37-40%)	20 mL
392 Glycerol	10 mL
393 Glacial acetic acid	10 mL
394 Absolute ethanol	30 mL
395 Distilled water	30 mL

396

397 Supplementary material 2. Paraformaldehyde fixing solution (100 mL) provided by the
398 platform of MNHN

399 Paraformaldehyde (16%)	25 mL
400 Glutaraldehyde (50%)	0.4 mL

Picric acid	0.1 mL
0.1M pH 7.4 Sorensen buffer	74.5 mL

Supplementary Table 1. The body weight of individual fish in different treatment groups

Group	Fish No.	Gender	Body weight (g)
MC-LR	1	Female	0.45
	2	Male	0.43
	3	Female	0.44
	4	Female	0.55
	5	Male	0.60
	6	Male	0.52
	7	Female	0.43
	8	Male	0.64
	9	Male	0.62
	10	Female	0.55
Non-toxin control	11	Male	0.43
	12	Female	0.55
	13	Male	0.59
	14	Female	0.50
Non-gavage control	15	Male	0.60
	16	Female	0.44

Figure descriptions:

Figure 1. Representative photos of histopathological observation of medaka liver under a light microscope.

A-D: resin sections (0.5 μm thick) of medaka liver with toluidine blue staining. Female control (A): abundant and distinct distribution of reserve vesicles (v); Females exposed to 10 $\mu g.g^{-1}$ bw of MC-LR (C): disintegration of the cord-like parenchymal organization, rounded hepatocytes containing various small bubbles (b), loss of reserve vesicles, nuclear membrane breakdown, chromatin concentration (c); Male control (B): abundant and distinct distribution of reserve vesicles (v); Males exposed to 10 $\mu g.g^{-1}$ bw of MC-LR (D): disintegration of the cord-like parenchymal organization, swollen and rounded hepatocytes, nuclear chromatin concentration (c), and increase in endoplasmic reticulum (e) and loss of nuclei (n). E-H: paraffin

418 sections (4 μm thick) of medaka liver with PAS staining. Female (E) and male (F)
419 control: abundant and distinct distribution of glycogen-reserve vesicles (red-purple);
420 Females (G) and males (H) exposed to 10 $\mu g.g^{-1}$ bw of MC-LR: less glycogen-reserve
421 vesicles compared with the control group.
422
423 Figure 2. Representative photos of immunolocalization of MC-LR in the liver and
424 gonad of toxin-treated fish through light microscopy.

425 Sections of the toxin-treated female liver (A), ovary (C), and testis (E), stained with
426 both toluidine blue and MC-LR immunolabeling (MC10E7), revealed with peroxidase
427 specific reaction of DAB. n, nucleus; h, hematoxylin; The secondary antibody control
428 sections of the toxin-treated female liver (B), ovary (D), and testis (F), stained with
429 toluidine blue; Sections of non-toxin control female liver (G), ovary (H), and testis (I),
430 stained with toluidine blue.
431
432 Figure 3. Representative photos of immunolocalization of MC-LR in the liver and
433 gonad of toxin-treated fish through immunogold electron microscopy.
434 The liver (A), ovary (E and G) and testis (I) of control fish: no clear immunolabeling.
435 The liver (B-D), ovary (F-H) and testis (J and K) of the fish exposed to 10 $\mu g.g^{-1}$ bw
436 of MC-LR, showing the immunolabeling of MC-LR indicated by the white arrow. For
437 liver, immunolabelings of MC-LR are clearly observed in the lytic residual (B) and
438 nuclear (C) of hepatocyte and the macrophage (D). For ovary, the immunolabeling is
439 found in the connective tissue (left) and the chorion (c) of the oocyte (right), as has
440 been shown in F, and less labelings are observed in the yolk vesicle (y) and the
441 cytoplasm (cy) of the oocyte (H). For testis, the labeling is intensively distributed in
442 some unidentified round structures, which appeared to be degenerated germ cells (J)
443 and the connective tissue of some certain area (K)
444

445 # Reference

446 Acuña, S., Baxa, D., Teh, S., 2012. Sublethal dietary effects of microcystin producing
447 *Microcystis* on threadfin shad, *Dorosoma petenense*. Toxicon 60, 1191–1202.
448 doi:10.1016/j.toxicon.2012.08.004
449 Campos, A., Vasconcelos, V., 2010. Molecular mechanisms of microcystin toxicity in
450 animal cells. Int. J. Mol. Sci. 11, 268–287. doi:10.3390/ijms11010268
451 Chen, J., Zhang, D., Xie, P., Wang, Q., Ma, Z., 2009. Simultaneous determination of
452 microcystin contaminations in various vertebrates (fish, turtle, duck and water
453 bird) from a large eutrophic Chinese lake, Lake Taihu, with toxic *Microcystis*
454 blooms. Sci. Total Environ. 407, 3317–3322.
455 doi:10.1016/j.scitotenv.2009.02.005
456 Dietrich, D.R., Krieger, H.O., 2009. Chapter 5. Male gonad anatomy and morphology,
457 in: Histological Analysis of Endocrine-Disruptive Effects in Small Laboratory
458 Fish. pp. 88–114.
459 Djediat, C., Malécot, M., de Luze, A., Bernard, C., Puiseux-Dao, S., Edery, M., 2010.
460 Localization of microcystin-LR in medaka fish tissues after cyanotoxin gavage.
461 Toxicon 55, 531–535. doi:10.1016/j.toxicon.2009.10.005
462 Djediat, C., Moyenga, D., Malécot, M., Comte, K., Yéprémian, C., Bernard, C.,
463 Puiseux-Dao, S., Edery, M., 2011. Oral toxicity of extracts of the
464 microcystin-containing cyanobacterium *Planktothrix agardhii* to the medaka fish
465 (*Oryzias latipes*). Toxicon 58, 112–122. doi:10.1016/j.toxicon.2011.05.011
466 Fischer, A., Hoeger, S.J., Stemmer, K., Feurstein, D.J., Knobeloch, D., Nussler, A.,
467 Dietrich, D.R., 2010. The role of organic anion transporting polypeptides

(OATPs/*SLCOs*) in the toxicity of different microcystin congeners *in vitro*: A comparison of primary human hepatocytes and OATP-transfected HEK293 cells. Toxicol. Appl. Pharmacol. 245, 9–20. doi:10.1016/j.taap.2010.02.006

Fischer, W.J., Altheimer, S., Cattori, V., Meier, P.J., Dietrich, D.R., Hagenbuch, B., 2005. Organic anion transporting polypeptides expressed in liver and brain mediate uptake of microcystin. Toxicol. Appl. Pharmacol. 203, 257–263. doi:10.1016/j.taap.2004.08.012

Fischer, W.J., Dietrich, D.R., 2000. Pathological and biochemical characterization of microcystin-induced hepatopancreas and kidney damage in carp (*Cyprinus carpio*). Toxicol. Appl. Pharmacol. 164, 73–81. doi:10.1006/taap.1999.8861

Fischer, W.J., Hitzfeld, B.C., Tencalla, F., Eriksson, J.E., Mikhailov, A., Dietrich, D.R., 2000. Microcystin-LR toxicodynamics, induced pathology, and immunohistochemical localization in livers of blue-green algae exposed rainbow trout (*oncorhynchus mykiss*). Toxicol. Sci. 54, 365–73. doi:10.1093/toxsci/54.2.365

Guzman, R.E., Solter, P.F., 2002. Characterization of sublethal microcystin-LR exposure in mice. Vet. Pathol. 39, 17–26. doi:10.1354/vp.39-1-17

Hagenbuch, B., Stieger, B., 2013. The SLCO (former SLC21) superfamily of transporters. Mol. Aspects Med. 34, 396–412. doi:10.1016/j.mam.2012.10.009

Hou, J., Li, L., Xue, T., Long, M., Su, Y., Wu, N., 2015. Hepatic positive and negative antioxidant responses in zebrafish after intraperitoneal administration of toxic microcystin-LR. Chemosphere 120, 729–736.

490 doi:10.1016/j.chemosphere.2014.09.079

491 Lance, E., Josso, C., Dietrich, D., Ernst, B., Paty, C., Senger, F., Bormans, M., Gérard,
492 C., 2010. Histopathology and microcystin distribution in *Lymnaea stagnalis*
493 (Gastropoda) following toxic cyanobacterial or dissolved microcystin-LR
494 exposure 98, 211–220.

495 Li, Y., Sheng, J., Sha, J., Han, X., 2008. The toxic effects of microcystin-LR on the
496 reproductive system of male rats *in vivo* and *in vitro*. Reprod. Toxicol. 26, 239–
497 245. doi:10.1016/j.reprotox.2008.09.004

498 MacKintosh, C., Beattie, K.A., Klumpp, S., Cohen, P., Codd, G.A., 1990.
499 Cyanobacterial microcystin-LR is a potent and specific inhibitor of protein
500 phosphatases 1 and 2A from both mammals and higher plants. FEBS 264, 187–
501 192.

502 Malbrouck, C., Kestemont, P., 2006. Effects of microcystins on fish. Environ. Toxicol.
503 Chem. 25, 72–86. doi:10.1897/05-029R.1

504 Marie, B., Huet, H., Marie, A., Djediat, C., Puiseux-Dao, S., Catherine, A., Trinchet,
505 I., Edery, M., 2012. Effects of a toxic cyanobacterial bloom (*Planktothrix*
506 *agardhii*) on fish: Insights from histopathological and quantitative proteomic
507 assessments following the oral exposure of medaka fish (*Oryzias latipes*). Aquat.
508 Toxicol. 114–115, 39–48. doi:10.1016/j.aquatox.2012.02.008

509 Mattos, L.J., Valença, S.S., Azevedo, S.M.F.O., Soares, R.M., 2014. Dualistic
510 evolution of liver damage in mice triggered by a single sublethal exposure to
511 Microcystin-LR. Toxicon 83, 43–51. doi:10.1016/j.toxicon.2014.02.015

512 Meier-Abt, F., Hammann-Hänni, A., Stieger, B., Ballatori, N., Boyer, J.L., 2007. The
513 organic anion transport polypeptide 1d1 (Oatp1d1) mediates hepatocellular
514 uptake of phalloidin and microcystin into skate liver. Toxicol. Appl. Pharmacol.
515 218, 274–279. doi:10.1016/j.taap.2006.11.015
516 Mezhoud, K., Bauchet, A.L., Château-Joubert, S., Praseuth, D., Marie, A., François,
517 J.C., Fontaine, J.J., Jaeg, J.P., Cravedi, J.P., Puiseux-Dao, S., Edery, M., 2008.
518 Proteomic and phosphoproteomic analysis of cellular responses in medaka fish
519 (*Oryzias latipes*) following oral gavage with microcystin-LR. Toxicon 51, 1431–
520 1439. doi:10.1016/j.toxicon.2008.03.017
521 Papadimitriou, T., Kagalou, I., Stalikas, C., Pilidis, G., Leonardos, I.D., 2012.
522 Assessment of microcystin distribution and biomagnification in tissues of aquatic
523 food web compartments from a shallow lake and evaluation of potential risks to
524 public health. Ecotoxicology 21, 1155–1166. doi:10.1007/s10646-012-0870-y
525 Puddick, J., Prinsep, M.R., Wood, S.A., Kaufononga, S.A.F., Cary, S.C., Hamilton,
526 D.P., 2014. High levels of structural diversity observed in microcystins from
527 *Microcystis* CAWBG11 and characterization of six new microcystin congeners.
528 Mar. Drugs 12, 5372–5395. doi:10.3390/md12115372
529 Qiao, Q., Le Manach, S., Huet, H., Duvernois-Berthet, E., Chaouch, S., Duval, C.,
530 Sotton, B., Ponger, L., Marie, A., Math??ron, L., Lennon, S., Bolbach, G.,
531 Djediat, C., Bernard, C., Edery, M., Marie, B., 2016. An integrated omic analysis
532 of hepatic alteration in medaka fish chronically exposed to cyanotoxins with
533 possible mechanisms of reproductive toxicity. Environ. Pollut. 219, 119–131.

534 doi:10.1016/j.envpol.2016.10.029

535 Schulz, R.W., de Fran??a, L.R., Lareyre, J.J., LeGac, F., Chiarini-Garcia, H., Nobrega,
536 R.H., Miura, T., 2010. Spermatogenesis in fish. Gen. Comp. Endocrinol. 165,
537 390–411. doi:10.1016/j.ygcen.2009.02.013

538 Shenolikar, S., 1994. Protein serine/threonine phosphatases - new avenues for cell
539 regulation. Annu. Biol. 10, 55–86.

540 Spoof, L., Catherine, A., 2017. Appendix 3: Tables of microcystins and nodularins, in:
541 Handbook of Cyanobacterial Monitoring and Cyanotoxin Analysis. pp. 526–537.
542 doi:10.1002/9781119068761.app3

543 Steiner, K., Hagenbuch, B., Dietrich, D.R., 2014. Molecular cloning and functional
544 characterization of a rainbow trout liver Oatp. Toxicol. Appl. Pharmacol. 280,
545 534–542. doi:10.1016/j.taap.2014.08.031

546 Steiner, K., Zimmermann, L., Hagenbuch, B., Dietrich, D., 2016. Zebrafish
547 Oatp-mediated transport of microcystin congeners. Arch. Toxicol. 90, 1129–
548 1139. doi:10.1007/s00204-015-1544-3

549 Su, Y., Li, L., Hou, J., Wu, N., Lin, W., Li, G., 2016. Life-cycle exposure to
550 microcystin-LR interferes with the reproductive endocrine system of male
551 zebrafish. Aquat. Toxicol. 175, 205–212. doi:10.1016/j.aquatox.2016.03.018

552 Trinchet, I., Cadel-Six, S., Djediat, C., Marie, B., Bernard, C., Puiseux-Dao, S., Krys,
553 S., Edery, M., 2013. Toxicity of harmful cyanobacterial blooms to bream and
554 roach. Toxicon 71, 121–127. doi:10.1016/j.toxicon.2013.05.019

555 Trinchet, I., Djediat, C., Huet, H., Dao, S.P., Edery, M., 2011. Pathological

556 modifications following sub-chronic exposure of medaka fish (*Oryzias latipes*)
557 to microcystin-LR. Reprod. Toxicol. 32, 329–340.
558 doi:10.1016/j.reprotox.2011.07.006
559 Wang, L., Wang, X., Geng, Z., Zhou, Y., Chen, Y., Wu, J., Han, X., 2013.
560 Distribution of microcystin-LR to testis of male Sprague-Dawley rats.
561 Ecotoxicology 22, 1555–1563. doi:10.1007/s10646-013-1141-2
562 Wang, X., Chen, Y., Zuo, X., Ding, N., Zeng, H., Zou, X., Han, X., 2013. Microcystin
563 (-LR) induced testicular cell apoptosis via up-regulating apoptosis-related genes
564 in vivo. Food Chem. Toxicol. 60, 309–317. doi:10.1016/j.fct.2013.07.039
565 Yoshida, T., Makita, Y., Tsutsumi, T., Nagata, S., Tashiro, F., Yoshida, F., Sekijima,
566 M., Tamura, S., Harada, T., Maita, K., Ueno, Y., 1998. Immunohistochemical
567 localization of microcystin-LR in the liver of mice: A study on the pathogenesis
568 of microcystin-LR-induced hepatotoxicity. Toxicol. Pathol. 26, 411–418.
569 doi:10.1177/019262339802600316
570 Yoshida, T., Tsutsumi, T., Nagata, S., Yoshida, F., Maita, K., Harada, T., Ueno, Y.,
571 2001. Quantitative analysis of intralobular distribution of microcystin-LR in the
572 mouse liver. J. Toxicol. Pathol. 14, 205–212. doi:10.1293/tox.14.205
573 Zeck, A., Eikenberg, A., Weller, M.G., Niessner, R., 2001. Highly sensitive
574 immunoassay based on a monoclonal antibody specific for [4-arginine]
575 microcystins. Anal. Chim. Acta 441, 1–13.
576 Zhang, H., Cai, C., Fang, W., Wang, J., Zhang, Y., Liu, J., Jia, X., 2013. Oxidative
577 damage and apoptosis induced by microcystin-LR in the liver of *Rana*

578 *nigromaculata* in vivo. Aquat. Toxicol. 140–141, 11–18.
579 doi:10.1016/j.aquatox.2013.05.009
580 Zhao, S., Xie, P., Li, G., Jun, C., Cai, Y., Xiong, Q., Zhao, Y., 2012. The proteomic
581 study on cellular responses of the testes of zebrafish (*Danio rerio*) exposed to
582 microcystin-RR. Proteomics 12, 300–312. doi:10.1002/pmic.201100214
583 Zhou, M., Tu, W.W., Xu, J., 2015. Mechanisms of microcystin-LR-induced
584 cytoskeletal disruption in animal cells. Toxicon 101, 92–100.
585 doi:10.1016/j.toxicon.2015.05.005
586 Zhou, Y., Chen, Y., Yuan, M., Xiang, Z., Han, X., 2013. In vivo study on the effects
587 of microcystin-LR on the apoptosis, proliferation and differentiation of rat
588 testicular spermatogenic cells of male rats injected i.p. with toxins. J. Toxicol.
589 Sci. 38, 661–70. doi:10.2131/jts.38.661
590 Zhou, Y., Yuan, J., Wu, J., Han, X., 2012. The toxic effects of microcystin-LR on rat
591 spermatogonia in vitro. Toxicol. Lett. 212, 48–56.
592 doi:10.1016/j.toxlet.2012.05.001
593

Figure 1

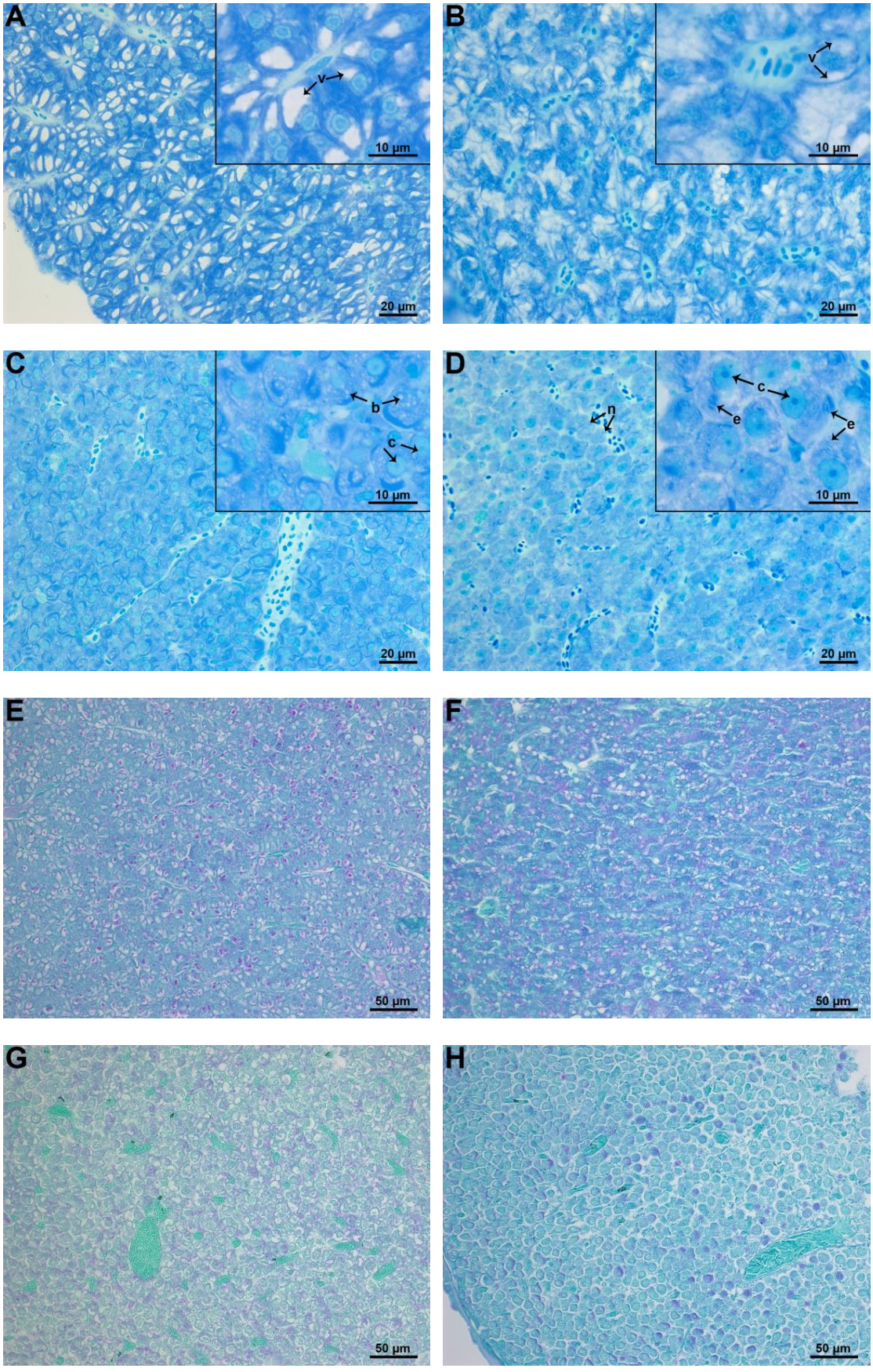

Figure 2

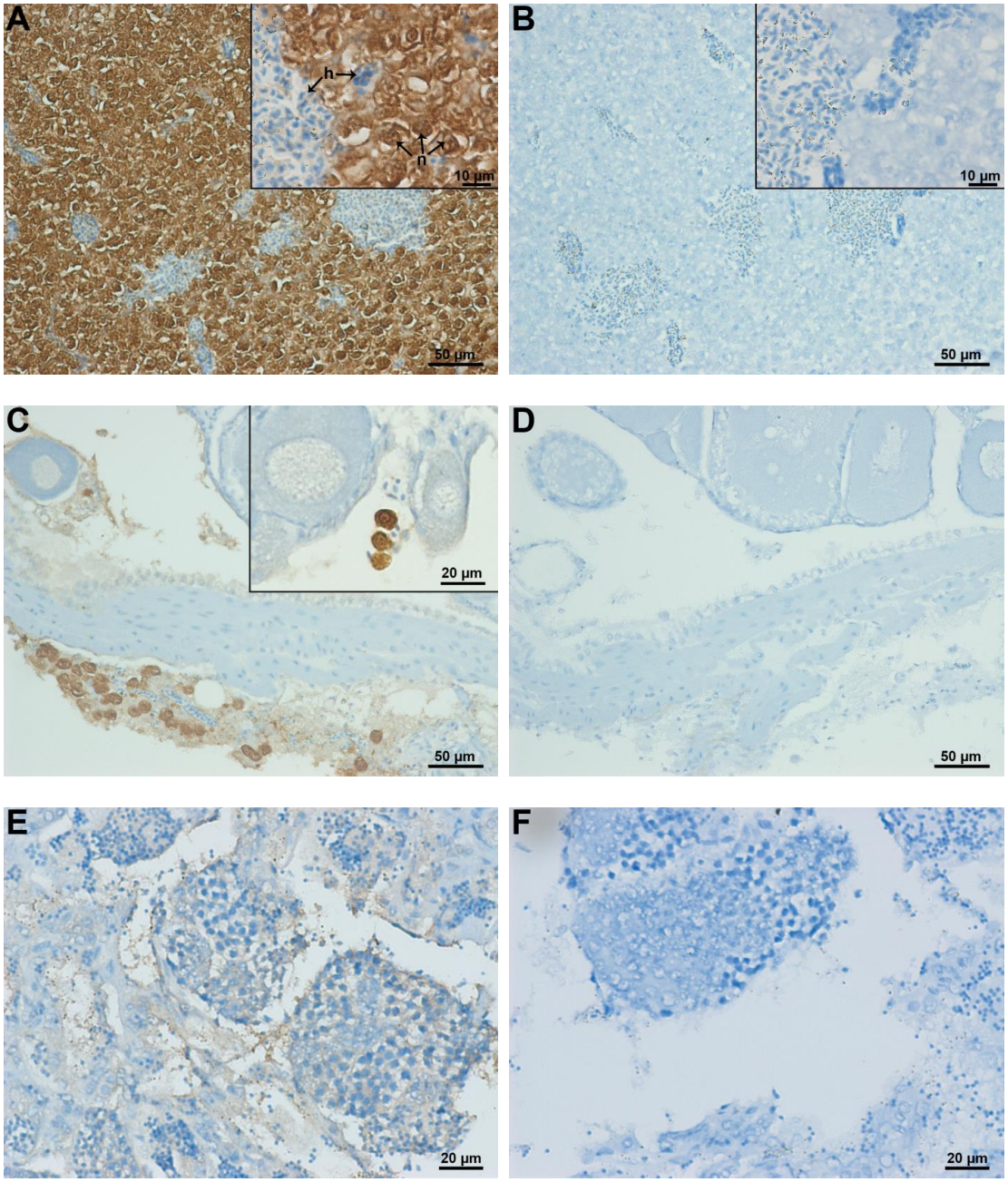

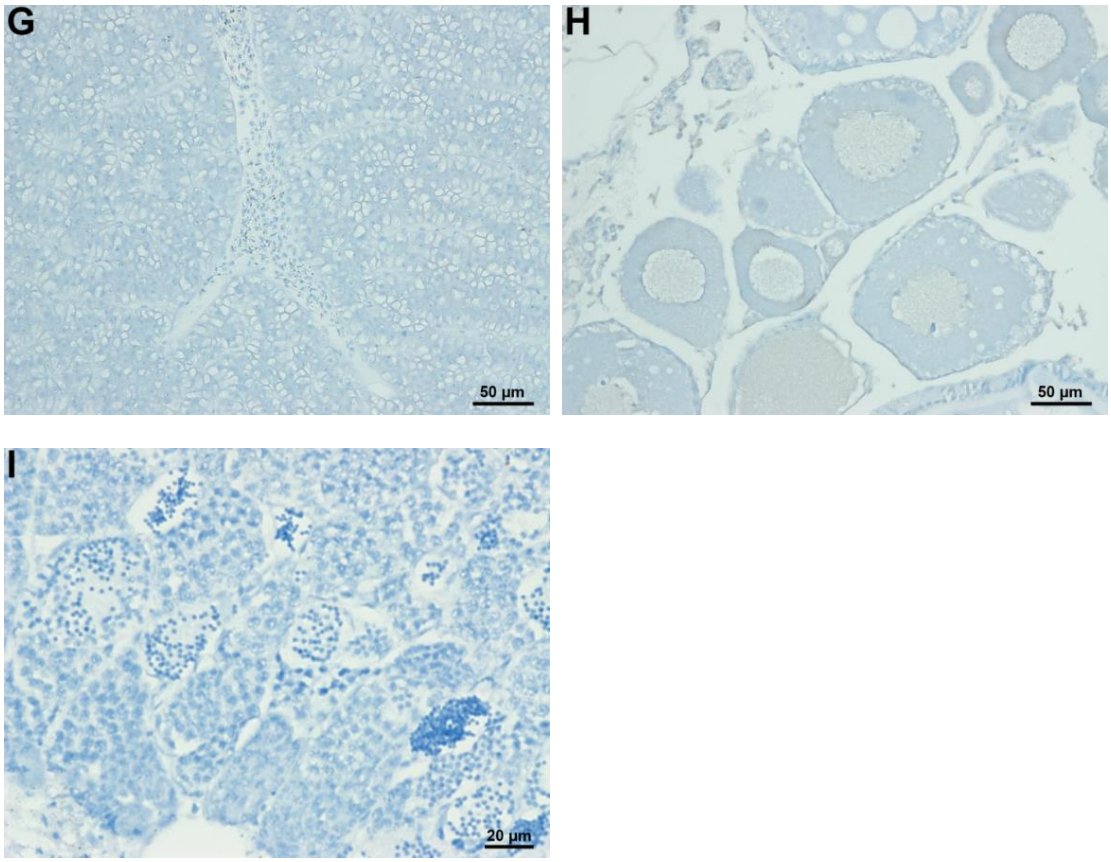

Figure 3